5. The size of the unbranched aliphatic chain determines the immunomodulatory potency of short and long-chain n-alkanols.

Damien Carignan, Olivier Désy, Manuel Caruso and Pedro O. de Campos-Lima*
Laval University Cancer Research Center, Quebec City, Quebec, G1R 2J6, Canada

* **Correspondence:** Dr. Pedro O. de Campos-Lima, Laval University Cancer Research Center, McMahon St 9, Quebec City, QC, G1R 2J6, Canada. Phone: 1 418 525 4444, fax: 1 418 691 5439, e-mail: pedro.campos-lima@crhdq.ulaval.ca

Short title: Immunomodulation by short and long-chain n-alkanols.

Keywords: n-alkanol, alcohol, immunomodulation, T cell, IFN-γ

Résumé

Les alcanols aliphatiques sont des substances ubiquitaires qui affichent des propriétés anesthésiques reliées à leur degré d'hydrophobicité. Une abondante littérature a documentée la capacité de l'éthanol, et d'autres alcools à courte chaîne, à modifier le système immunitaire en interférant avec la fonction de plusieurs types de cellules. Nous avons pensé que, puisque les *n*-alcanols aliphatiques non-ramifiés sont structurellement très similaires, ils pourraient avoir un impact immunologique qui réflète leur puissance anesthésique. Dans cet article, nous rapportons l'impact de la série homologue des alcools de C_1 à C_{12} sur la capacité des lymphocytes primaires humains à produire de l'IFN-γ une fois activé par leur récepteur à l'antigène. Le méthanol a accru la production d'IFN-γ tandis que les alcools de C_2 à C_{10} ont réduit la sécrétion de cette cytokine. L'activité de la série des *n*-alcanols a été observée sur une très large gamme de concentrations allant de niveaux de l'ordre des mM pour les alcools à chaîne courte jusqu'à des niveaux de l'ordre des μM pour les alcools C_9-C_{10}. Nous avons observé une corrélation claire entre l'activité immunomodulatrice et l'hydrophobicité des composés, mais un effet de coupure était évident à C_{11}. Les *n*-alcanols ont agit en aval de la membrane cellulaire puisque la signalisation précoce associée au récepteur à l'antigène a été préservée. L'activation du facteur de transcription NFAT est progressivement altérée en fonction de la taille de la chaîne aliphatique des *n*-alcanols en suivant une tendance claire vers le bas qui éa été interrompue à C_{11}. L'activation de la voie NF-κB est aussi affectée par les *n*-alcanols, mais leur effet s'arrête avant, aux environs de C_8. Le patron de la dérégulation transcriptionnelle et de l'immunomodulation induite par la série des *n*-alcanols suggère la présence de poches d'intéraction de dimensions définies sur des cibles protéiques intracellaires qui compromettent l'activation de NFAT et NF-κB et, finalement modulent la fonction effectrice des lymphocytes T. Ce travail contribue à une meilleure compréhension de l'activité biologique des alcanols.

Abstract

Aliphatic n-alkanols are ubiquitous substances that display general anesthetic properties in accordance to their degree of hydrophobicity. Extensive literature has documented the capacity of ethanol and other short-chain alcohols to modulate the immune system by interfering with the function of several types of immune cells. We reasoned that because unbranched aliphatic n-alkanols are structurally very similar they might have an immunological impact that mirrors their anesthetic potency. In this article, we report the impact of the homologous C_1-C_{12} alcohol series on the ability of human primary lymphocytes to produce IFN-γ once activated by the T cell receptor. Methanol enhanced IFN-γ production while C_2-C_{10} alcohols reduced the release of this cytokine. The activity of the n-alkanol series was observed within a very wide concentration window ranging from mM levels for short-chain alcohols to μM amounts in the case of C_9-C_{10} alcohols. There was a clear correlation between immunomodulatory activity and hydrophobicity of the compounds but a cutoff effect was evident at C_{11}. n-Alkanols were shown to act downstream of the cell membrane because T cell receptor early signaling was preserved. The activation of the nuclear factor of activated T cells (NFAT) was down-regulated progressively in accordance to the size of the n-alkanol aliphatic chains with a clear downward trend that was interrupted at C_{11}. The nuclear factor-κB (NF-κB) signaling was also compromised but the cutoff appeared earlier in the vicinity of C_8. The pattern of immunomodulation and transcriptional dysregulation induced by the n-alkanol series suggested the existence of interaction pockets of defined dimensions within intracellular targets that compromise the activation of NFAT and NF-κB transcription factors and ultimately modulate the effector function of the T lymphocyte. This work contributes to a better understanding of the biological activity of n-alkanols.

Introduction

Aliphatic n-alkanols constitute a large family of ubiquitous substances composed of short-chain (C_1-C_5) and long-chain (C_6-C_{22}) alcohols that are used in a variety of domestic and

industrial applications (Désy *et al.*, 2012; Veenstra, 2009). Extensive literature has documented the capacity of ethanol to modulate the immune system directly or indirectly by interfering with the function of T lymphocytes, monocytes, macrophages, dendridic cells, neutrophils, and endothelial cells (Goral and Kovacs, 2005; Oak *et al.*, 2006; Saeed *et al.*, 2004; Szabo *et al.*, 2007; Taieb *et al.*, 2002; Zhao *et al.*, 2003). Recent results have provided evidence that two other short-chain alcohols also possess a discernible immunomodulatory footprint. Thus, isopropanol was shown to down-regulate the effector function of T cells, NK cells and monocytes (Désy *et al.*, 2008; Carignan *et al.*, 2012). Conversely, methanol enhances the inflammatory cytokine release from activated T lymphocytes (Désy *et al.*, 2010). A common thread in the mechanisms that underlie the biological effect of the above short-chain alcohols is their obvious impact on transcriptional pathways that are important for immune cell function. Many of the effects of ethanol on the immune system have been associated to the dysfunctional activation of the nuclear factor-κB (NF-κB) (Oak *et al.*, 2006; Saeed *et al.*, 2004; Szabo *et al.*, 2007), and at least in lipopolysaccharide-activated macrophages, these biological consequences have been suggested to result from a change in the dynamics of protein recruitment into rafts on the cell membrane (Dai *et al.*, 2005; Szabo *et al.*, 2007). Instead, the impact of isopropanol and methanol initiates downstream of the cell membrane and is mediated by the dysregulation of distinct members of the nuclear factor of activated T cells (NFAT) family of transcription factors with or without additional involvement of the activator protein-1 (AP-1) (Désy *et al.*, 2012).

The work described in this article was set off by two observations: first, unbranched aliphatic n-alkanols display general anesthetic properties that correlate with their degree of hydrophobicity (McCreery and Hunt 1978; Pringle *et al.*, 1981; Franks and Lieb 1984, 1985); and second, our own preliminary data shows that isopropanol is substantially more effective than ethanol in down-regulating the effector function of T lymphocytes. We reasoned that because unbranched aliphatic n-alkanols are structurally very similar they might have an immunological impact that mirrors their anesthetic potency observed within the C_1-C_{12} range. We have chosen the production of IFN-γ by human primary T lymphocytes as the readout to test our hypothesis because this cytokine is essential for the

innate and adaptive immune response (Billiau and Matthys 2009). The present article reports that indeed the size of the aliphatic chains determines the immunomodulatory potency of n-alkanols. Furthermore, our results suggest the existence of discrete molecular targets downstream of the cell membrane, which display defined alcohol interaction cutoffs.

Materials and Methods

Cell isolation, culture, and stimulation. This study was approved by the Institutional Clinical Research Ethics Committee (L'Hôtel-Dieu de Québec/Centre hospitalier universitaire de Québec - L'HDQ-CHUQ). Mononuclear cells were prepared from the peripheral blood from healthy volunteers by density gradient centrifugation using Ficoll-Hypaque (GE Healthcare, Piscataway, NJ). Written informed consent was obtained from all donors. Monocyte-depleted populations were more than 95% pure human T cells ($CD8^+/CD4^+$) and were kept in complete medium: RPMI 1640 (Invitrogen Canada, Burlington, Canada) supplemented with 10% heat-inactivated FBS (BioCell Inc., Drummondville, Canada).

T cells were activated with anti-CD3/CD28 antibody-coated magnetic beads (Invitrogen) at 37°C for 6 h. When indicated, three alternative T cell activation protocols were used: (i) Pre-treatment for 20 min on ice with 1 μg/mL mouse anti-human CD3 monoclonal antibody (CD3-2, Mabtech, Nacka Strand, Sweden) and 2.5 μg/mL mouse anti-human CD28 (CD28.2, Biolegend, San Diego, CA), followed by incubation at 37°C for 3 min with a 10-fold excess of goat anti-mouse IgG (Sigma); (ii) Treatment was identical to the one described in (i) except for the incubation step at 37°C that was performed for 5 h; and (iii) Treatment with 10 ng/ml phorbol 12-myristate 13-acetate (PMA) and 200 ng/ml ionomycin (Sigma, St Louis, MO) for 5 h.

Alcohols. 99.9% Methanol (C_1) was purchased from Fisher Scientific, Pittsburgh, PA, USA. > 99% pure Ethanol (C_2) was purchased from Commercial Alcohols, Brampton,

Canada. 99.5% 1-butanol (C_4) was purchased from BDH (Toronto, Canada). 99.9% 1-propanol (C_3), 99% 1-pentanol (C_5), 99% 1-hexanol (C_6), 99% 1-heptanol (C_7), 99% 1-octanol (C_8), 98% 1-nonanol (C_9), 99% 1-decanol (C_{10}), 99% 1-undecanol (C_{11}), and 98% 1-dodecanol (C_{12}) were purchased from Alfa-Aesar, Ward Hill, MA, USA. A two- to five-times concentrated stock solution of C_1-C_7 alcohols was prepared in serum-free RPMI and diluted to the final experimental concentration. For C_8-C_{12} alcohols, a stock solution was first prepared in DMSO and further diluted in assay medium to the desired experimental concentration with extensive vortexing. The final DMSO concentration was never higher than 0.2%.

Cytokine analysis. Measurements of human IFN-γ in cell culture supernatants were performed with the ELISA MAX™ Standard kit according to the manufacturer's instructions (BioLegend). Supernatants from human cells were diluted 1:100; thus, only negligible alcohol amounts were still present at the time of processing of diluted supernatants. These trace quantities had no impact on the assay itself. Briefly, 96-well plates were coated with the relevant capture antibody and incubated with serially diluted standards or unknown samples; then, they were washed and incubated with the biotinylated detection antibody followed by streptavidin-horseradish peroxidase. The plates were read at 450 nm after sequential treatment with 3,3',5,5'-tetramethylbenzidine (TMB) substrate solution and phosphoric acid.

ELISA-Based Transcription Factor Activation Assay. Cells were washed in alcohol-free buffer before the generation of nuclear lysates. Nuclear proteins were extracted using the Active Motif Nuclear Extract Kit (Active Motif, Carlsbad, CA) according to the manufacturer's instructions; the total protein concentration of the lysates was determined by the Bradford assay (Bio-Rad, Hercules, CA). p65 activation was measured with the ELISA-based TransAM NF-κB Kit by following to the manufacturer's instructions (Active Motif). Briefly, nuclear extracts were incubated with plate-bound p65–specific oligonucleotides; the plates were washed and further incubated with p65–specific antibodies. Addition of a horseradish-conjugated secondary antibody and the 3,3',5,5'-

tetramethylbenzidine substrate produced a colorimetric reaction measurable in a spectrophotometer.

Western blot. For ZAP-70 analysis, purified T cells were activated for 3 minutes at 37°C by anti-CD3/anti-CD28/anti-IgG antibodies as described above with or without the relevant alcohol at the indicated molar concentration. The cells were washed in alcohol-free buffer and lysed in sodium dodecyl sulfate (SDS) sample buffer (2% w/v SDS, 0.25 M β-mercaptoethanol, 10% v/v glycerol, 0.05 M Tris-HCl, pH 6.8, 0.004% w/v bromophenol blue); lysates were separated in 10% polyacrylamide gels and blotted onto nitrocellulose filters (Hybond-C, GE Healthcare, Piscataway, NJ). The membranes were first probed with ZAP-70-specific antibodies: rabbit anti-human ZAP-70 (99F2, 1/1000, Cell Signaling Technology, Danvers, MA) and mouse anti-human ZAP-70 (pY319)/Syk (pY352) (17a, 1/5000, BD Biosciences, Mississauga, Canada); For NFATc1 analysis, purified T cells were activated for 5 h by PMA/ionomycin as described above with or without the relevant alcohol at the indicated molar concentration. Nuclear extracts were prepared with the Active Motif kit; samples were separated in 7.5% polyacrylamide gels and blotted onto nitrocellulose filters (Hybond-C, GE Healthcare, Piscataway, NJ). The membranes were first probed with mouse anti-human NFATc1 monoclonal antibody (7A6, 1/500, Biolegend) and rabbit anti-human HDAC1 polyclonal antibody (H-51, 1/2000, Santa Cruz Biotechnology, Santa Cruz, CA).

Blots were then washed and incubated with 1/15000 dilutions of the antibodies IRDye 680 goat anti-rabbit IgG and IRDye 800CW goat anti-mouse IgG (Li-Cor Biosciences, Lincoln, NE). Detection and quantification was performed with the Odyssey Infrared Imaging System (Li-Cor Biosystems).

Luciferase assay. The generation of Jurkat cells carrying the firefly luciferase gene driven by the NFAT synthetic promoter is described elsewhere (Désy et al., 2008). The stable Jurkat cell line expressing the constitutive luciferase was produced by transduction with an MFG vector that carries the luciferase gene driven by the Moloney murine leukemia virus long terminal repeat (LTR) (Qiao et al. 2002). Jurkat cells carrying the inducible or

constitutive luciferase were stimulated with PMA/ionomycin with or without methanol treatment as indicated in the text. Lysates for luciferase assays were prepared with the passive lysis buffer (E1941; Promega, Madison, WI) and analyzed in a Lumat 9501 luminometer (Berthold, Nashua, NH). Relative luciferase units were calculated in relation to the unstimulated negative control after normalization to total protein content measured by the Bradford assay (Bio-Rad).

Statistical analysis. One-way ANOVA followed by Dunnett's multiple-comparison posttest was performed with GraphPad Prism (GraphPad Software Inc., San Diego, CA) on data presented in table 5.1 and figure 5.3. p values < 0.05 were considered significant.

Results

Primary alcohols modulate the secretion of interferon-γ by human primary lymphocytes according to the size of their aliphatic chain

One major effector function of T cells triggered by the engagement of their antigen receptor is the synthesis of IFN-γ (Billiau and Matthys 2009). In the present study, we have investigated whether exposure *in vitro* to a panel of primary aliphatic alcohols spanning the C_1-C_{12} range would have any impact on the ability of human primary lymphocytes to produce IFN-γ once activated by the T cell receptor. Preliminary assays were performed to determine the optimal concentration window for analysis of each alcohol, which were then tested in 3-6 independent experiments with cells isolated from different donors. Table 5.1 illustrates the results obtained with five alcohol concentration points starting from no alcohol (group 0) to the highest concentration (group IV). The mean viability of cells exposed to the highest concentration of each alcohol was always > 97% as indicated. Three distinct outcomes were observed. As anticipated, the release of IFN-γ was up-regulated by methanol exposure with about 70% increase measured in the culture supernatants by ELISA at the highest alcohol concentration. In contrast, T lymphocytes treated with C_2-C_{10}

alcohols produced lower amounts of this cytokine, with inhibition levels of 68-96% recorded at the highest concentration tested. C_{11}-C_{12} alcohols had little or no impact on IFN-γ secretion and the only significant effect was observed with the highest 1-undecanol concentration, which led to 30% reduction in cytokine release.

The biological effect of alcohols is also depicted in figure 5.1. Upon examination of the plotted curves, it becomes apparent that although all C_2-C_{10} alcohols exhibit a clear inhibitory impact on IFN-γ production, they do so at very different concentrations in accordance with the size of their carbon chain. Thus, short-chain alcohols are effective in low mM levels, while C_9-C_{10} alcohols work at μM amounts.

The homologous series of primary alcohols has an immunomodulatory activity profile with a plateau in the mid range and a discrete cutoff effect

It is well established that the anesthetic potency of the homologous series of primary alcohols as measured by the loss of the righting reflex in tadpoles exhibits progressive intensity that parallels the increase in size of their carbon chains. This pattern, however, is abruptly interrupted at C_{12} with substantial loss of activity at C_{13} and the observation of a virtual disappearance of activity at C_{14} and longer alcohols (Pringle *et al.*, 1981). In addition, the potency levels off at C_6-C_7 in a lipid-free *in vitro* model of anesthetic-protein interaction (Franks and Lieb, 1985, 2004). In order to better characterize the profile of immunomodulatory activity of the alcohol series and to verify how close it resembles the pattern of anesthetic potency, the concentration values associated to 50% of the biological effect of each alcohol were calculated from the corresponding curves in figure 5.1 and then plotted against the maximal achievable concentration in aqueous media in figure 5.2. The 50% effect was generally within each experimental curve; in the case of C_{11}, the last experimentally achievable data point corresponded to 30% inhibition and higher concentrations were beyond its maximal solubility. C_{12} was totally ineffective. In agreement with the data obtained in the studies on anesthetic potency, examination of the resulting curve for the immunomodulatory potency of primary alcohols revealed a qualitative match with a plateau at C_5-C_6 and a cutoff at C_{11}.

The homologous series of primary alcohols shares the lack of impact on early signaling events triggered by activation of the T cell receptor

Our previous work has shown that methanol and isopropanol initiate their biological effect downstream of the cell membrane in lymphocytes (Désy *et al.*, 2008, 2010). It remained possible, however, that the longer C_4-C_{11} alcohols would act on the cell membrane in a way reminiscent of the effect of ethanol on ion channels and neurotransmitter receptors (Jung *et al.*, 2005; Aryal *et al.*, 2009). In this scenario, longer n-alkanols could plausibly interact with the T cell receptor directly and blunt antigen-dependent signal transduction. We have tested this possibility by checking the phosphorylation status of ZAP-70, a major player in early T cell signaling. As shown in figure 5.3, none of the C_4-C_{11} alcohols interferes with signaling through the T cell receptor as demonstrated by their lack of effect on ZAP-70 activation following anti-CD3 antibody cross-linking. A similar picture was obtained by the analysis of a downstream target of ZAP-70, the *Linker of Activated T Cells* or LAT, whose phosphorylation was not affected by the above n-alkanols (data not shown).

The homologous series of primary alcohols reduce the activation and nuclear content of the nuclear factor of activated T cells in primary human lymphocytes according to the length of their aliphatic chains

We have previously shown that the secondary alcohol isopropanol mediates the attenuation of lymphocyte effector functions, including the capacity to secrete IFN-γ, by down-regulating the activation of NFATc1. As the experiments reported here revealed that primary alcohols with aliphatic chains spanning C_2-C_{11} similarly reduce IFN-γ production in human primary lymphocytes, the underlying dysregulation of the activation of this transcription factor was a plausible assumption. We have set out to examine this possibility by measuring NFATc1 in nuclear lysates from lymphocytes that have been activated in the presence of each one of the various n-alkanols. Moreover, we have chosen to activate the T cells with a stimulus that bypasses the membrane to further corroborate the view that the studied chemicals work without relying on early TCR signaling. Indeed, the Western blot analysis in figure 5.4, panel A, shows that ionophore-activated lymphocytes display lower amounts of nuclear NFATc1 when exposed to n-alkanols. The concentrations used were

those capable of inducing 75% of the biological effect as measured by IFN-γ secretion and ranged from mM amounts for the short-chain molecules to μM levels for the longer moieties as described in the figure legend. NFATc1 levels in C_7-C_{10}-treated samples hovered around half the maximal content of activated T cells (55.8% for C_7, 50.8% for C_8, 54% for C_9, 58.8% C_{10}). This inhibitory activity on NFATc1 activation was not significantly found in activated lymphocytes exposed to C_{11}, which exhibited close to 75% of the maximal content of activated T cells.

Next, we have confirmed the above results by using a more sensitive luciferase assay with a stable T cell line carrying an NFAT-responsive promoter. This time we have activated the T cells through the antigen and co-stimulatory receptors with anti-CD3/CD28 antibody-coated beads. Figure 5.4, panel B, shows a significant downward trend in promoter activity (ANOVA $p < 0.0001$) that parallels the increase in size of the alcohol aliphatic chains. The percentage inhibition of NFAT activation measured in this assay was 34.2%, 36.6%, 48.2%, 57.4%, 53.4%, and 56.5% for C_6, C_7, C_8, C_9, C_{10}, and C_{11}, respectively.

It is noteworthy that alkanols may directly affect the luciferase activity in certain experimental conditions. However, we have conducted the luciferase assays in absence of alkanols with lysates prepared from washed cells. Moreover, to further validate our results, we have tested the effect of each alcohol on a stable T cell line that carries an integrated cassette in which the luciferase gene is driven by a constitutive promoter. Figure 5.4, panel C, shows that C_1-C_9 and C_{12} did not change the constitutive luciferase activity in our experimental conditions. Instead, we noticed that C_{10} and C_{11} change the luciferase activity, and C_{10} did so significantly. Thus, in the specific case of C_{10} and C_{11}, the luciferase assay is not conclusive as to their impact on NFAT activation. However, the Western blot analysis in figure 5.4, panel A, complements these results by revealing that C_{10} does indeed reduce NFATc1 in the nucleus.

Similarly to the Western blot analysis, the alcohol concentrations used in the luciferase assays were progressively lower so that the longer the alcohol the lower the amount needed to produce the observed effect. Given the higher sensitivity of the luciferase assay, we have chosen the concentrations that are depicted in figure 5.2, which are required to produce 50% of the biological effect as measured by IFN-γ release in lymphocytes. Thus, while C_6

reduced the NFAT-responsive promoter activity by one third, the dampening effect of C_9 reached about 60%. Nevertheless, 1.4 mM of C_6 and only 106 μM of C_9 were needed to produce this outcome, thereby stressing the higher potency of the long-chain molecules.

Nuclear translocation of the nuclear factor-κB is affected by n-alkanols in activated T cells

Although the dysregulation of the nuclear factor-κB (NF-κB) signaling cascade seems to play an important part in the immunological effects of ethanol, we have previously found that this pathway is not altered in the case of two other short-chain alcohols, methanol and isopropanol. In order to dissect further the immunomodulation mechanism of the homologous series of primary alcohols, we have measured the nuclear translocation of p65 in TCR-stimulated purified human T cells exposed to the same alcohol concentrations previously used for Western blot analysis. The p65 protein is the Rel transactivating component of the major and most common NF-κB heterodimer.

Figure 5.5 shows that lymphocyte activation by anti-CD3/CD28 antibodies led to a 1.6-fold increase in the amount of p65 in the nucleus. Conversely, the same stimulation in the presence of 860 μM C_7 barely moved the p65 nuclear content, leading to a dismal increase that represented 12.8% of the maximal p65 nuclear content above the unstimulated cell baseline. The effect of the homologous series of primary alcohols was dependent on the size of the aliphatic chain and produced a V shaped curve with the highest inhibition observed in the middle for C_6-C_8 and little or no effect detected for C_1-C_3 on the one end and C_{11}-C_{12} on the other.

Discussion

This article reports three novel findings: (i) the immunomodulatory capacity of the homologous series of n-alkanols displays a clear correlation to hydrophobicity and is reminiscent of their well-established general anesthetic potency; (ii) the pattern of immunomodulatory activity of the alcohol series suggests the existence of an interaction pocket of defined dimensions; and (iii) the immunomodulatory target(s) of n-alkanols is

(are) located downstream of the cell membrane.

Most of the research on the mechanism of action of alcohols and other general anesthetics had first been focused on the cell membrane and finds its roots in the independent contributions of Hans H. Meyer and Charles E. Overton over a century ago (Meyer 1899; Overton 1901). Their seminal work established the basis for one of the most tested correlations in biomedicine, namely, that between anesthetic potency of a given compound and its oil: water partition coefficient. In face of the strong experimental evidence in support of this correlation, it was natural to assume that anesthetics (and by extension alcohols) would work under a unifying theory in which the dissolution of lipophilic molecules in the lipid bilayer could modify its physical properties and compromise indirectly the function of embedded proteins (Eckenhoff 2001; Seeman 1972). Nevertheless, several incongruities have cast doubts about the validity of the different flavors of the lipid theory to explain the mechanism of action of alcohols and anesthetics (Franks and Lieb 1982). To single out a few, alcohol-induced changes in lipid phase transitions are minute and comparable in magnitude to the effect of mild hyperthermia, which obviously lacks the consequences predicted by the lipid theory (Eckenhoff 2001). Another inconsistence was revealed by the finding of substantial differences in biological activity between stereoisomers that are supposed to have the same impact on lipid phase transition (Dickinson et al., 2000). Also, a cutoff effect was evident when a homologous series of n-alkanols (or n-alkanes) was tested with increasing anesthetic activity being observed up to a discrete alcohol size after which it disappeared even though the larger ineffective molecules were highly lipophilic (Franks and Lieb 1985). Finally, compounds that possess high lipid solubility and fail to display anesthetic activity regardless of their size have been described in obvious discordance with the central tenet of the lipid theory (Koblin *et al.*, 1994).

On the one hand, our results indicate that the Meyer-Overton correlation do apply to the alcohol immunomodulatory activity, but on the other hand, they do not lend support to the interpretation that membrane alterations are the major underlying process. First, there is a clear cutoff effect, and second, the inability of these molecules, including the longer more hydrophobic C_9-C_{10} alcohols, to change ZAP-70 phosphorylation strongly suggests that by

whatever means they operate they do so downstream of the cell membrane.

Previous studies reported putative alcohol-binding sites in several proteins, and there are now crystallographic data for some of them, including ion channels, enzymes, and the odorant binding protein LUSH (Franks et al., 1998; Kruse et al., 2003; Nury et al., 2011; Pegan et al., 2006; Ramaswamy et al., 1994). A feature that was consistently found in these structural analyses of the alcohol-binding site was the identification of hydrogen bond acceptor site(s) and of a hydrophobic groove in close vicinity (Désy *et al.*, 2012). Thus, it is plausible to interpret the Meyer-Overton correlation without resorting to lipid solubility if one applies their concept to the context of hydrophobic protein subdomains. In this scenario, alcohols or similar molecules would dislodge water from hydrophobic pockets and use hydrogen bonds and van der Waals forces to stabilize their binding with potential conformational and functional consequences (Klemm 1998). The hydrophobic nature of the molecules would still dictate the outcome of the interaction and the volume constraints of the relevant cavities would account for the cutoff effect. It is noteworthy that about half of the molecular mass of the cell membrane is in fact protein (Eckenhoff 2001). Nevertheless, at least in principle, all cellular compartments could provide suitable protein targets for alcohols.

One of the first and arguably most convincing pieces of evidence that proteins may be the actual mechanistic targets of alcohol action is the demonstrated ability of the homologous series of primary alkanols to inhibit luciferase activity *in vitro* in absence of a lipid context (Franks and Lieb 1984, 1985). These experiments revealed an almost linear correlation between luciferase inhibition and general anethestic potency. Alcohols were shown to inhibit luciferase activity progressively better from C_1 to C_6 and then from C_8 to C_{12}; there was a clear cutoff effect at C_{16} and two identifiable activity plateaus between C_6-C_7 and between C_{12}-C_{16} in which the binding affinity was nearly the same. These findings implied the existence of a hydrophobic binding pocket in the enzyme with sufficient volume to lodge two 1-hexanol molecules or a single 1-dodecanol molecule (Franks and Lieb 2004). Subsequent X-ray structural studies confirmed the existence of specific binding sites that coincide with the substrate-binding pocket (Franks *et al.*, 1998). There is a striking similarity between the overall profile of the immunomodulatory activity of primary

alcohols reported here and that associated to their ability to inhibit luciferase (Franks and Lieb 1985). In both situations, there was a first inflection in the response curve, which leveled off in the mid range at C_5-C_6 in our case (Fig. 5.2). A second inflection appeared at C_{10} in our case and at C_{12} for luciferase. There was no obvious leveling off of the immunomodulatory activity before or after this point as opposed to the plateau of luciferase activity observed at C_{12}-C_{16}. In both cases, however, the second inflection led to the crossing of the maximum solubility curve at C_{11} and C_{16}, exactly where the cutoff points for IFN-γ production and luciferase activity have been experimentally determined to occur, respectively. The analysis of the results reported here and the analogy to the luciferase inhibition data permit us to predict that the alcohol immunomodulatory effect is mediated by the alteration of one (and conceivably more than one) intracellular protein target via interaction to a hydrophobic pocket. This cavity is likely to be sufficiently big to accommodate two molecules of 1-pentanol, as suggested by the leveling off of IFN-γ release in the mid-range of the curve depicted in figure 5.2, or a single molecule of 1-decanol. Additional methyl groups are likely to contribute to the binding energy by augmenting the van der Waals interactions up to C_5. From this point on, two molecules would be too big to fit simultaneously and part of their aliphatic chains would remain exposed to the external polar environment. Efficient binding of single molecules would drive the increase in potency from C_7-C_{10} but steric constraints would resume at C_{11}. It is noteworthy that the amount of C_{11} required to produce 30% inhibition, which is within the soluble range, is comparable to the concentration of C_{10} that induces the same biological effect as can be inferred from table 5.1. The complete loss of activity at higher concentrations, however, is not necessarily due to molecular size but to solubility. The immunomodulatory cutoff is lower than that observed for anesthetic potency or for luciferase activity (Franks and Lieb 1985; Pringle *et al.*, 1981), suggesting that the interaction occurs within a somewhat smaller cavity.

Given that early signaling seems to be preserved in the presence of all alcohols tested here (fig. 5.3) and that our previous work on short-chain alcohols has shown their exquisite specificity in inducing the dysregulation of transcription factors that play a role in the activation of immunologically relevant genes (Désy *et al.*, 2008, 2010), we favor the

hypothesis that the putative intracellular targets are the transcription factors themselves or molecules placed immediately upstream in their signaling cascades. The linear correlation between the size of the aliphatic chain and NFAT inhibition within the C_2-C_{10} range and the loss of activity at C_{11} are reminiscent of the findings obtained with IFN-γ release and support the previous assumption of existence of a pocket sufficiently large to accommodate C_{10}. In the case of NF-κB, the results obtained in the p65 activation experiments are compatible with the existence of an additional alcohol-binding site of smaller dimensions within a member of this activation pathway whose maximal capacity would fit C_7 or C_8. The reduced NF-κB activation would synergize with NFAT inhibition, notably between C_6-C_8. The combined end result of n-alkanol action on these two transcriptional pathways would be the progressive disablement of immune cell function between C_2-C_{10} and loss of effect at C_{11}-C_{12}.

The analysis of figure 5.1 shows a clear dichotomy between the pattern of response elicited by methanol and that triggered by all the other n-alcohols. Either methanol binds to the same pocket but produces a different conformational change or, perhaps, its smaller size and lower hydrophobicity allow binding to different molecular structures in the same or in a distinct set of targets. In any case, the crystal structure of bromoform bound to luciferase demonstrates that a molecule not much bigger than methanol with a single carbon atom is capable of binding the same cavities that accommodate longer alcohols (Franks et al., 1998).

The data reported in this article have confirmed our original hypothesis and revealed that all primary alcohols have an immunological impact that mirrors their anesthetic potency. This effect correlates well with hydrophobicity but the site of their action does not involve the membrane. The discrete alcohol modulation cutoff and the general profile of the IFN-γ release curve suggest the binding to a hydrophobic pocket in a common intracellular protein target. NFATc1 is a conceivable candidate, whose activation is inhibited by alcohols in a way that closely resembles the reduction in IFN-γ production and exhibits a similar cutoff. Moreover, our data also reveals an additional target in the NF-κB pathway with an earlier cutoff, whose inhibition could synergize with the NFATc1 down-regulation in the nucleus and ultimately reduce IFN-γ release. The biological effect of alcohols,

encompassing the anesthetic and immunomodulatory properties, may result from interactions with many potential molecular targets that display suitable hydrophobic cavities. It is also likely to depend on cell type- and activation state-dependent protein expression profiles. Thus, in principle, our results should be interpreted within the context of the activation of human primary T cells through their antigen receptor. Altogether, our work contributes to a better understanding of the biological activity of the ubiquitous family of n-alkanols and provides additional insight into the mechanism that underlies their impact on the function of T lymphocytes in particular.

Acknowledgements

The authors wish to thank S. Comeau and H. Dombrowski for blood collection. The authors declare no financial or commercial conflict of interest. This work was supported by grants from the National Sciences and Engineering Research Council of Canada (327062-07) and the Canada Foundation for Innovation (4087) to P.O.d.C.-L.

References

Aryal, P., Dvir, H., Choe, S., Slesinger, P.A. (2009). A discrete alcohol pocket involved in GIRK channel activation. *Nat. Neurosci.* **12,** 988-995.

Bell, G.H. (1973). Solubilities of normal aliphatic acids, alcohols and alkanes in water. Chem. Phys. Lipids **10,** 1-10.

Billiau, A., Matthys, P. (2009). Interferon-gamma: a historical perspective. *Cytokine Growth Factor Rev.* **20,** 97-113.

Carignan, D., Désy, O., de Campos-Lima, P.O. (2012). The dysregulation of the monocyte/macrophage effector function induced by isopropanol is mediated by the defective activation of distinct members of the AP-1 family of transcription factors. *Toxicol. Sci.* **125**:144-156.

Dai, Q., Zhang, J., Pruett, S. B. (2005). Ethanol alters cellular activation and CD14 partitioning in lipid rafts. *Biochem. Biophys. Res. Commun.* **332,** 37-42.

Désy, O., Carignan, D., Caruso, M., de Campos-Lima, P. O. (2008). Immunosuppressive

effect of isopropanol: down-regulation of cytokine production results from the alteration of discrete transcriptional pathways in activated lymphocytes. *J. Immunol.* **181,** 2348-2355.

Désy, O., Carignan, D., Caruso, M., de Campos-Lima, P. O. (2010). Methanol induces a discrete transcriptional dysregulation that leads to cytokine overproduction in activated lymphocytes. *Toxicol. Sci.* **17,** 303-313.

Désy, O., Carignan, D., de Campos-Lima, P.O. (2012). Short-term immunological effects of non-ethanolic short-chain alcohols. *Toxicol. Lett.* **210:**44-52.

Dickinson, R., White, I., Lieb, W.R., Franks, N.P. (2000). Stereoselective loss of righting reflex in rats by isoflurane. *Anesthesiology* **93,** 837–843.

Eckenhoff, R.G. (2001). Promiscuous ligands and attractive cavities: how do the inhaled anesthetics work? *Mol. Interv.* **1,** 258-268.

Franks, N.P., Jenkins, A., Conti, E., Lieb, W.R., Brick, P. (1998). Structural basis for the inhibition of firefly luciferase by a general anesthetic. *Biophys. J.* **75,** 2205-2211.

Franks, N.P., Lieb, W.R. (1982). Molecular mechanisms of general anaesthesia. *Nature* **300,** 487-493.

Franks, N.P., Lieb, W.R. (1984). Do general anaesthetics act by competitive binding to specific receptors? *Nature* **310,** 599-601.

Franks, N.P., Lieb, W.R. (1985). Mapping of general anaesthetic target sites provides a molecular basis for cutoff effects. *Nature* **316,** 349-351.

Franks, N.P., Lieb, W.R. (2004). Seeing the light: protein theories of general anesthesia. *Anesthesiology* **101,** 235-237.

Goral, J., Kovacs, E. J. (2005). In vivo ethanol exposure down-regulates TLR2, TLR4, and TLR9-mediated macrophage inflammatory response by limiting p38 and ERK1/2 activation. *J. Immunol.* **174,** 456-463.

Jung, S., Akabas, M. H., Harris, R. A. (2005). Functional and structural analysis of the $GABA_A$ receptor alpha 1 subunit during channel gating and alcohol modulation. *J. Biol. Chem.* **280,** 308-316.

Klemm, W.R. (1998). Biological water and its role in the effects of alcohol. *Alcohol* **15,** 249-267.

Koblin, D.D., Chortkoff, B.S., Laster, M.J., Eger, E.I. 2nd, Halsey, M.J., Ionescu, P. (1994). Polyhalogenated and perfluorinated compounds that disobey the Meyer-Overton hypothesis. *Anesth. Analg.* **79,** 1043–1048.

Kruse, S.W., Zhao, R., Smith, D.P., Jones, D.N. (2003). Structure of a specific alcohol-binding site defined by the odorant binding protein LUSH from Drosophila melanogaster. *Nat. Struct. Biol.* **10,** 694-700.

McCreery, M.J., Hunt, W.A., (1978). Physico-chemical correlates of alcohol intoxication. *Neuropharmacology* **17,** 451-461.

Meyer, H.H. (1899). Zur Theorie der Alkoholnarkose. Erste Mittheilung. Welche Eigenschaft der Anästhetica bedingt ihre narkotische Wirkung? *Arch. Exp. Pathol. Pharmakol.* **42,** 109-118.

Nury, H., Van Renterghem, C., Weng, Y., Tran, A., Baaden, M., Dufresne, V., Changeux, J.P., Sonner, J.M., Delarue, M., Corringer, P.J. (2011). X-ray structures of general anaesthetics bound to a pentameric ligand-gated ion channel. *Nature* **469,** 428-431.

Oak, S., Mandrekar, P., Catalano, D., Kodys, K., Szabo, G. (2006). TLR2- and TLR4-mediated signals determine attenuation or augmentation of inflammation by acute alcohol in monocytes. *J. Immunol.* **176,** 7628-7635.

Overton, E. (1901). Studien über die Narkose, Zugleich ein Beitrag zur allgemeinen Pharmakologie. Gustav Fischer, Jena, Germany.

Pegan, S., Arrabit, C., Slesinger, P.A., Choe, S. (2006). Andersen's syndrome mutation effects on the structure and assembly of the cytoplasmic domains of Kir2.1. *Biochemistry* **45,** 8599-8606.

Pringle, M.J., Brown, K.B., Miller, K.W. (1981). Can the lipid theories of anesthesia account for the cutoff in anesthetic potency in homologous series of alcohols? *Mol. Pharmacol.* **19,** 49-55.

Qiao, J., Roy, V., Girard, M.H., Caruso, M. (2002). High translation efficiency is mediated by the encephalomyocarditis virus internal ribosomal entry sites if the natural sequence surrounding the eleventh AUG is retained. *Hum. Gene Ther.* **13,** 881-887.

Ramaswamy, S., Eklund, H., Plapp, B.V. (1994). Structures of horse liver alcohol dehydrogenase complexed with NAD+ and substituted benzyl alcohols. *Biochemistry*

33, 5230-5237.

Saeed, R. W., Varma, S., Peng, T., Tracey, K. J., Sherry, B., Metz, C. N. (2004). Ethanol blocks leukocyte recruitment and endothelial cell activation in vivo and in vitro. *J. Immunol.* **173,** 6376-6383.

Seeman, P. (1972). The membrane actions of anesthetics and tranquilizers. *Pharmacol. Rev.* **24,** 583-655.

Szabo, G., Dolganiuc, A., Dai, Q., Pruett, S. B. (2007). TLR4, ethanol, and lipid rafts: a new mechanism of ethanol action with implications for other receptor-mediated effects. *J. Immunol.* **178,** 1243-1249.

Taieb, J., Delarche, C., Ethuin, F., Selloum, S., Poynard, T., Gougerot-Pocidalo, M. A., Chollet-Martin, S. (2002). Ethanol-induced inhibition of cytokine release and protein degranulation in human neutrophils. *J. Leukoc. Biol.* **72,** 1142-1147.

Veenstra, G., Webb, C., Sanderson, H., Belanger, S.E., Fisk, P., Nielsen, A., Kasai, Y., Willing, A., Dyer, S., Penney, D., Certa, H., Stanton, K., Sedlak, R. (2009). Human health risk assessment of long chain alcohols. *Ecotoxicol. Environ. Saf.* **72,** 1016-1030.

Zhao, X. J., Marrero, L., Song, K., Oliver, P., Chin, S. Y., Simon, H., Schurr, J. R., Zhang, Z., Thoppil, D., Lee, S., Nelson, S., Kolls, J. K. (2003). Acute alcohol inhibits TNF-alpha processing in human monocytes by inhibiting TNF/TNF-alpha-converting enzyme interactions in the cell membrane. *J. Immunol.* **170,** 2923-2931.

Table 5.1 - Correlation between primary alcohol carbon-chain length and T lymphocyte IFN-γ release[§]

CONCENTRATION GROUP[#]	1-OH	2-OH	3-OH	4-OH	5-OH	6-OH	7-OH	8-OH	9-OH	10-OH	11-OH
0	101 ± 2	105 ± 6.7	98.2 ± 4	88.8 ± 2.4	100.3 ± 7	105.2 ± 0.7	100.7 ± 1.9	119.9 ± 8.1	99.7 ± 3.4	109.6 ± 4.1	107.7 ± 7.9
I	122 ± 7.5 *ns*	110.6 ± 7.6 *ns*	73.1 ± 8.6 *ns*	78.8 ± 3.1 *ns*	70.5 ± 8.3*	80.8 ± 4.9**	75.1 ± 5**	58.9 ± 7.6**	82.3 ± 3.2*	96.5 ± 4.8 *ns*	91.3 ± 6.5 *ns*
II	134 ± 3 *ns*	89.2 ± 11.6 *ns*	60.9 ± 8.7**	50.4 ± 2.7**	46.9 ± 5.4**	60.2 ± 4.4**	51.1 ± 4**	44.6 ± 7.8**	76.2 ± 3.1**	83.6 ± 2.5**	90.7 ± 4.9 *ns*
III	158.6 ± 14*	42.7 ± 3.9**	46.9 ± 13.4**	25.7 ± 3.7**	23.5 ± 4.9**	24.1 ± 3.6**	24.8 ± 3.9**	20.5 ± 2.4**	55 ± 4.7**	59.9 ± 4**	84.7 ± 8 *ns*
IV	167 ± 19.8**	3.4 ± 2.4**	13.4 ± 4.1**	13.4 ± 4**	11.7 ± 3.8**	7 ± 2.7**	8.2 ± 4.2**	3.4 ± 1.4**	32.4 ± 7.3**	22.9 ± 3**	69.8 ± 3.4**
% VIABILITY[∫∫]	98.9 ± 0.8	99.2 ± 0.2	98.9 ± 0.1	99.2 ± 0.4	97.5 ± 1.6	99.8 ± 0.2	98.9 ± 0.1	99.3 ± 0.3	98.9 ± 1.1	99.4 ± 0.6	99.4 ± 0.6

T cells were activated by anti-CD3/anti-CD28 antibodies in the absence of alcohols (group 0) or in the absence of alcohols and the presence of 0.2% DMSO (DMSO). Alternatively, T cells were activated by anti-CD3/anti-CD28 antibodies in the presence of the indicated alcohols (groups I-IV). Group I represents the lowest and group IV the highest tested alcohol concentrations with intermediary ascending values in the groups in-between. The experimental molar concentration for each alcohol was: *Group I* (1-OH, 23.4 mM; 2-OH, 12.5 mM; 3-OH, 6.2 mM; 4-OH, 2.0 mM; 5-OH, 1134 μM; 6-OH, 489 μM, 7-OH, 215.1 μM; 8-OH, 96 μM; 9-OH, 21.7 μM; 10-OH, 14.6 μM; 11-OH, 29 μM); *Group II* (1-OH, 46.8 mM; 2-OH, 25 mM; 3-OH, 6.7 mM; 4-OH, 2.4 mM; 5-OH, 1418 μM; 6-OH, 979 μM, 7-OH, 430.3 μM; 8-OH, 192 μM; 9-OH, 43.3 μM; 10-OH, 29.2 μM; 11-OH, 43.5 μM); *Group III* (1-OH, 93.6 mM; 2-OH, 50 mM; 3-OH, 7.5 mM; 4-OH, 2.7 mM; 5-OH, 1700 μM; 6-OH, 1958 μM, 7-OH, 860.6 μM; 8-OH, 384 μM; 9-OH, 86.7 μM; 10-OH, 58.4 μM; 11-OH, 58 μM); and *Group IV* (1-OH, 187 mM; 2-OH, 100 mM; 3-OH, 8.3 mM; 4-OH, 3.0 mM; 5-OH, 1985 μM; 6-OH, 3915 μM, 7-OH, 1721 μM; 8-OH, 768 μM; 9-OH, 173.3 μM; 10-OH, 116.9 μM; 11-OH, 75.4 μM). The results for 12-OH are not shown because there was no effect at all tested concentrations, including that corresponding to its maximal aqueous solubility.

§ Data are shown as percentage of the IFN-γ release from the TCR-activated DMSO control. Means ± SEM are indicated (*ns:* $p > 0.05$, * $p < 0.05$, ** $p < 0.01$ relative to group 0; n: 3 for 1-OH, 2-OH, 8-OH, 10-OH and 11-OH; n: 4 for 4-OH, 5-OH and 9-OH; n: 6 for 3-OH, 6-OH and 7-OH).

∬ Viability was assessed after exposure to the highest alcohol concentration.

Figure symbols: 1-OH (C_1), methanol; 2-OH (C_2), ethanol; 3-OH (C_3), 1-propanol; 4-OH (C_4), 1-butanol; 5-OH (C_5), 1-pentanol; 6-OH (C_6), 1-hexanol; 7-OH (C_7), 1-heptanol; 8-OH (C_8), 1-octanol; 9-OH (C_9), 1-nonanol; 10-OH (C_{10}), 1-decanol; 11-OH (C_{11}), 1-undecanol; 12-OH (C_{12}), 1-dodecanol.

Figures and Legends

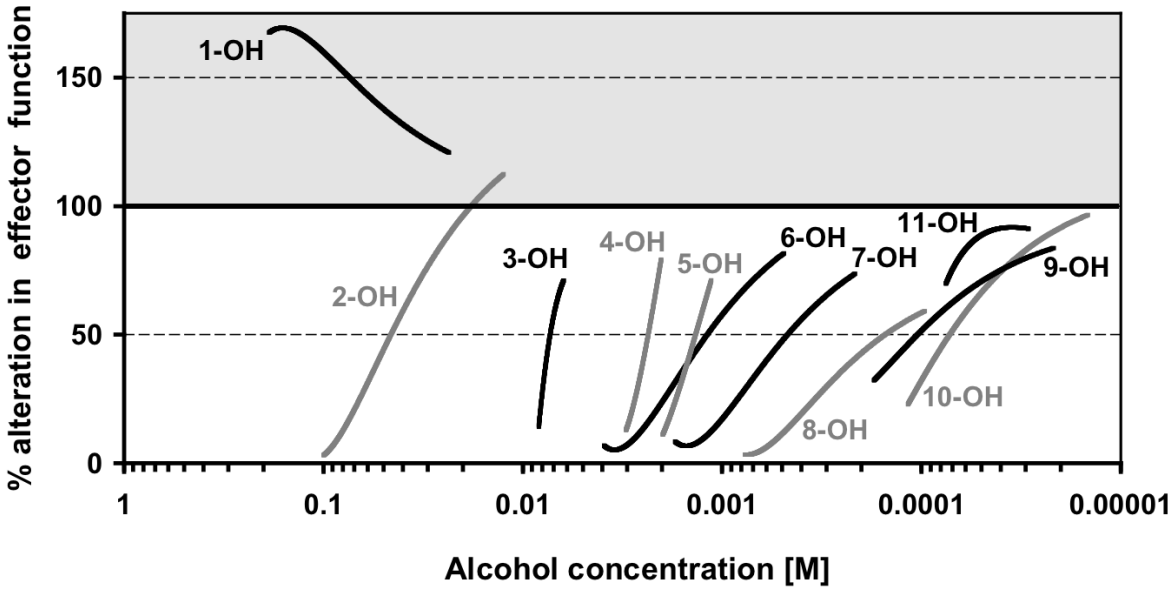

Figure 5.1 - Individual profiles of the immunomodulatory activity of primary alcohols.

Primary alcohols alter IFN-γ production in peripheral blood T lymphocytes: Purified T cells were stimulated with anti-CD3/CD28 antibody-coated beads for 6 h in the presence of C_1-C_{12} alcohols within the molar concentration windows indicated. The IFN-γ levels released in the supernatants were measured by ELISA and used to calculate the % alteration in effector function in relation to the positive control activated in absence of alcohols (100%). Resulting data indicating inhibition of IFN-γ release for C_2-C_{11} or enhancement of IFN-γ production for C_1 are depicted in the form of curves. The corresponding data points are shown in table 1 and were compiled from independent experiments with samples from at least three different donors for each alcohol as detailed in the table footnote. Panel symbols: *1-OH,* C_1, methanol; *2-OH,* C_2, ethanol; *3-OH,* C_3, 1-propanol; *4-OH,* C_4, 1-butanol; *5-OH,* C_5, 1-pentanol; *6-OH,* C_6, 1-hexanol; *7-OH,* C_7, 1-heptanol; *8-OH,* C_8, 1-octanol; *9-OH,* C_9, 1-nonanol; *10-OH,* C_{10}, 1-decanol; *11-OH,* C_{11}, 1-undecanol.

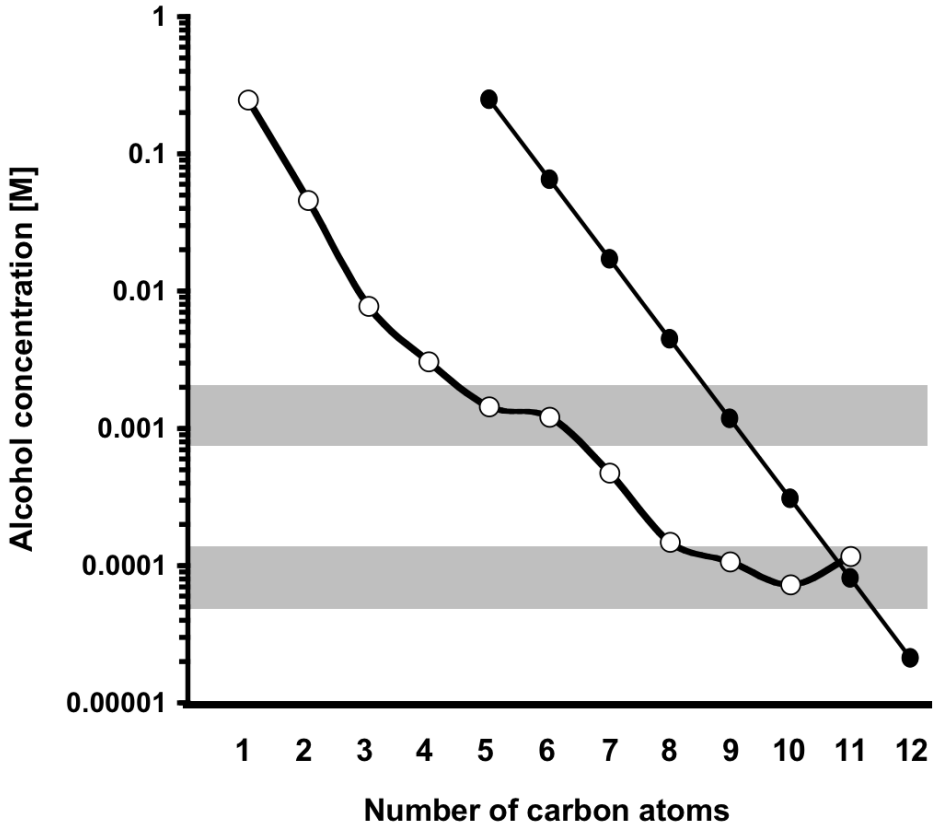

Figure 5.2 - Collective profile of the immunomodulatory activity of the homologous series of primary alcohols.

The concentrations required to induce 50% of the immunomodulatory effect were calculated from individual response curves for each alcohol and are depicted as linked empty circles. The maximal aqueous solubility for C_5-C_{12} alcohols was plotted as filled circles in a straight line following the equation described by Bell (Bell 1973). The curve inflections are inside grey boxes. The number of carbons identifies the alcohols.

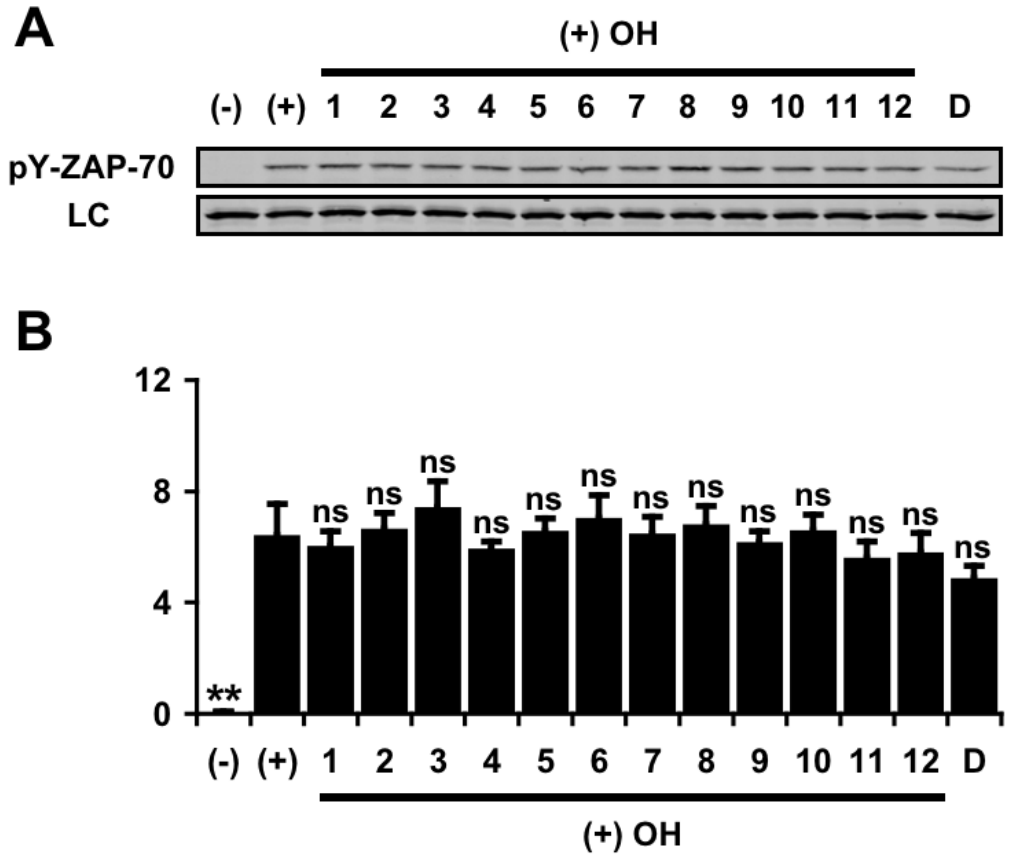

Figure 5.3 - Primary alcohols and TCR early signaling.

Treatment with primary alcohols does not affect ZAP-70 phosphorylation following TCR activation: Peripheral blood T cells were stimulated for 3 min with anti-CD3/CD28/anti-IgG in the absence or the presence of each alcohol at the concentrations that produce 75% of the biological effect as measured by IFN-γ release (augmentation for C_1 and inhibition for C_2-C_{10}). The chosen concentrations for C_2-C_{10} were: C_1:, C_2:, C_3:, C_4:, C_5:, C_6:, C_7:, C_8:, C_9:, C_{10}:, C_{11}:, C_{12}:. The maximal water soluble concentrations were used in the case of C_{11}-C_{12},, respectively. Samples were processed for SDS/PAGE and one representative blot of three is shown. Relative quantification in relation to total ZAP-70 is presented underneath as mean densitometric units ± SEM; *ns:* $p > 0.05$, ** $p < 0.01$, n: 3. None of the alcohols had an effect on ZAP-70 phosphorylation in absence of TCR stimulation (not shown).

Figure symbols: (-), unstimulated cells in the absence of alcohols; (+), TCR-stimulated cells in the absence of alcohols. TCR-activated samples treated with alcohols are indicated by their number of carbons (1-12). LC: Loading control (Total ZAP-70). OH: Alcohol.

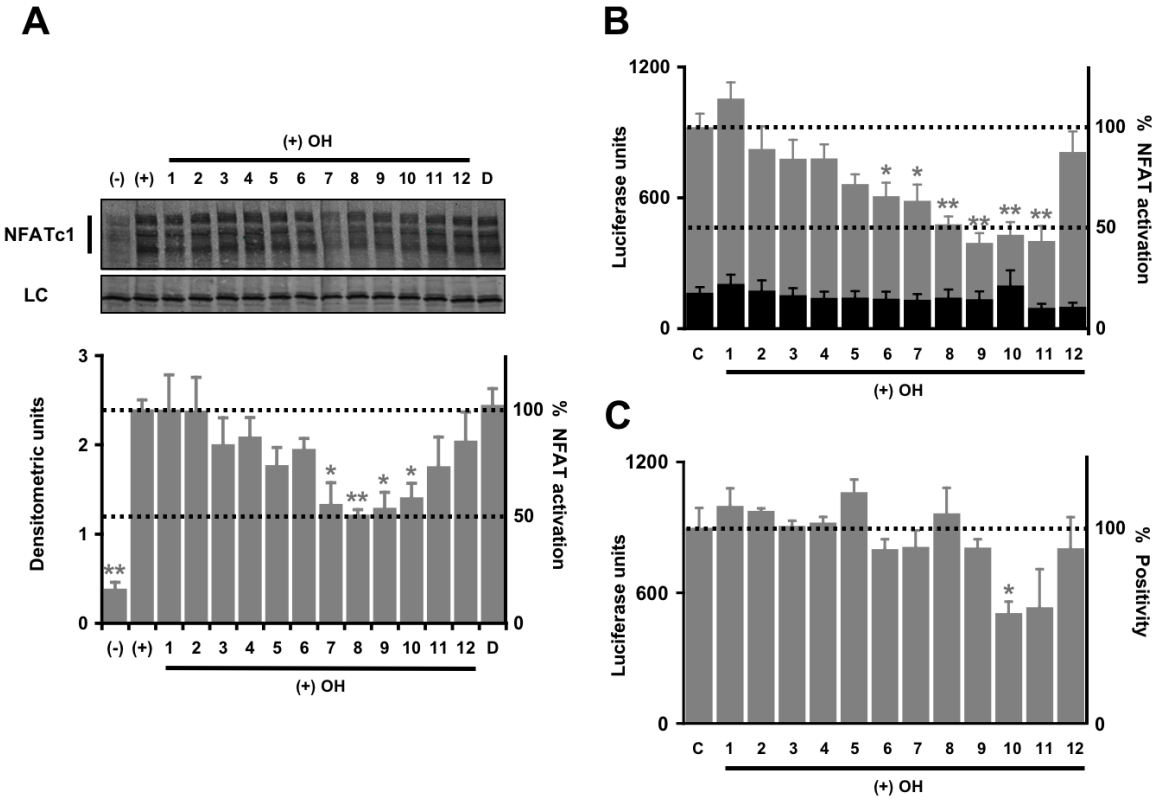

Figure 5.4 - Primary alcohols affect NFAT activation.

(A) Measurement of NFATc1 in the nucleus by Western blot. Human peripheral blood T cells were stimulated with PMA/ionomycin for 5 hours in the presence or absence of the relevant alcohol. The chosen concentration for each alcohol were those capable of inducing 75% of the biological effect or the maximal water soluble amount as described in the legend of figure 3. Nuclear extracts were prepared from each sample and processed for SDS/PAGE; one representative blot of four is shown. Relative quantification in relation to histone deacetylase (HDAC-1) is presented underneath as mean densitometric units ± SEM; * $p < 0.05$, ** $p < 0.01$ relative to the (+) control group, n: 4. Non significant values, $p > 0.05$, are not labeled.

The relative NFATc1 content in relation to the (+) control group is also presented as % values. The mean of the (+) control group, which represents 100%, and the 50% value are indicated by dashed lines.

(B) A) Primary alcohols modulate the activation of a synthetic promoter containing NFAT

binding sites. Jurkat-luciferase cells were stimulated with anti-CD3/CD28 antibody-coated beads for 5 h in presence or absence of the relevant alcohol. Grey columns show TCR-activated samples. Black columns represent unstimulated samples. The concentrations used in the experiments were those capable of inducing 50% of the biological effect as measured by IFN-γ release for C_2-C_{10} or those representing the maximal water solubility for C_{11}-C_{12} (Figure 2). Samples were lysed and assayed for luciferase activity. Results are presented as mean relative luciferase units per microgram of protein ± SEM; * $p < 0.05$, ** $p < 0.01$ relative to the (+) control group, n: 6. Non significant values, $p > 0.05$, are not labeled.
The relative NFATc1 activation in relation to the (+) control group is also presented as % values. The mean of the (+) control group, which represents 100%, and the 50% value are indicated by dashed lines.
(C) Impact of primary alcohols on the enzymatic activity of constitutively expressed luciferase. A stable Jurkat subclone carrying the luciferase gene driven by the Moloney LTR was stimulated by anti-CD3/CD28 antibody-coated beads for 5 h in the presence of the same alcohol concentrations used in panel B. Samples were lysed and assayed for luciferase activity. Results are presented as mean relative luciferase units per microgram of protein ± SEM; * $p < 0.05$ relative to the (+) control group, n: 3. Non significant values, $p > 0.05$, are not labeled. The relative luciferase activity is also presented as % values in relation to the (+) control group. The mean of the (+) control group, which represents 100%, is indicated by a dashed line.

Figure symbols: (-), unstimulated cells in absence of alcohols; (+), TCR-stimulated cells in absence of alcohols. TCR-activated samples treated with alcohols are indicated by their number of carbons (1-12). D: TCR-stimulated cells in the absence of alcohols and in the presence of 0.2% DMSO. LC: Loading control (HDAC-1). OH: Alcohol.

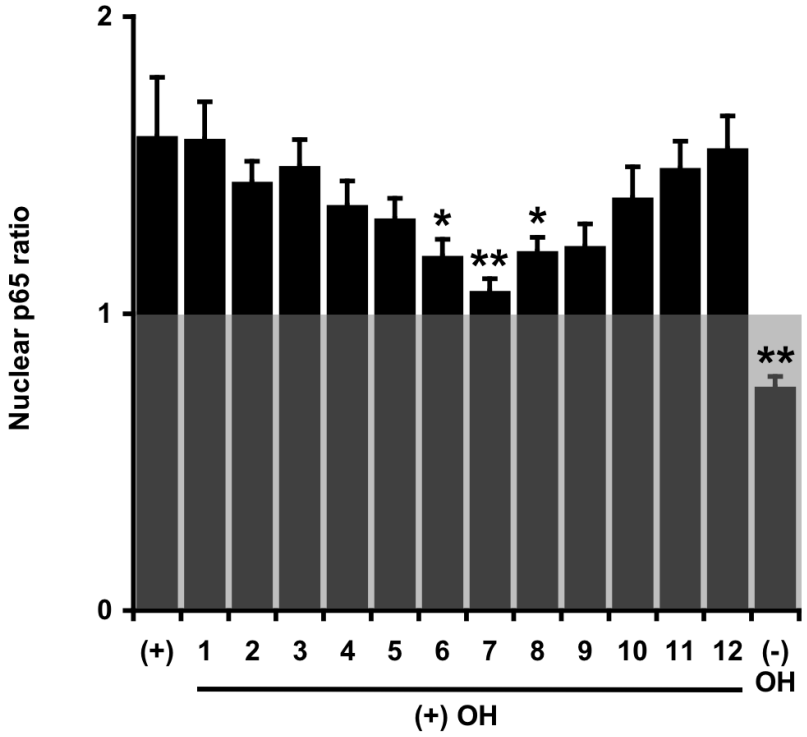

Figure 5.5 - Impact of primary alcohols on NF-κB activation in human primary lymphocytes

Treatments with C6-C8 primary alcohols inhibit NF-κB activation following TCR activation: Peripheral blood T cells were stimulated for 5 h with anti-CD3/anti-IgG in the absence or the presence of each alcohol at the concentrations that produce 75% of the biological effect as measured by IFN-γ release. The relevant concentrations are listed in the legend of figure 3.

Nuclear extracts were incubated with immobilized p65-binding oligonucleotides in 96-well plates; the amount of retained transcription factor was assessed with a p65-specific antibody by ELISA. The nuclear p65 ratio was calculated by dividing the sample value by the value of the unstimulated control in absence of alcohols. Data are presented as means ± SEM; * $p < 0.05$, ** $p < 0.01$ relative to the (+) control group, n: 5. Non significant values, $p > 0.05$, are not labeled.

Figure symbols: (+), TCR-stimulated cells in absence of alcohols. (-)OH, unstimulated cells in absence of alcohols and in the presence of C_7 (C_7 was chosen as a representative alcohol

because it is placed in the middle of the alcohol series). TCR-activated samples treated with alcohols are indicated by their number of carbons (1-12). OH: Alcohol.